



A significant diurnal pattern of ammonia dry deposition to a cropland is detected by an open-path quantum cascade laser-based eddy covariance instrument

Kai Wang^{a,1}, Jingxia Wang^{b,1}, Zhichen Qu^b, Wen Xu^b, Kai Wang^b, Hongyan Zhang^b, Jianlin Shen^c, Peng Kang^d, Xiaojie Zhen^e, Yin Wang^d, Xunhua Zheng^a, Xuejun Liu^{b,*}

^a State Key Laboratory of Atmospheric Boundary Layer Physics and Atmospheric Chemistry, Institute of Atmospheric Physics, Chinese Academy of Sciences, Beijing, 100029, China

^b National Academy of Agriculture Green Development, Key Laboratory of Plant-Soil Interactions of MOE, College of Resources and Environmental Sciences, China Agricultural University, Beijing, 100193, China

^c Key Laboratory of Agro-ecological Processes in Subtropical Region and Changsha Research Station for Agricultural & Environmental Monitoring, Institute of Subtropical Agriculture, Chinese Academy of Sciences, Changsha, 410125, China

^d HealthyPhoton Co., Ltd., Ningbo, 315105, China

^e Jiangsu Tynoo Corporation, Wuxi, 214021, China

HIGHLIGHTS

- The open-path QCL-based eddy covariance instrument can detect small NH₃ fluxes.
- Nitrogen loss rate from the wheat field through NH₃ volatilization was 0.57–0.71%.
- NH₃ dry deposition averaged to 0.014 kg N ha⁻¹ d⁻¹ with a significant diurnal pattern.
- Depositions estimated by inferential model were two times larger than the observed.

ARTICLE INFO

Keywords:

Ammonia
Ammonia volatilization
Dry deposition
Eddy covariance
Open-path analyzer
Cropland

ABSTRACT

Large uncertainties and challenges remain in the quantification of land-atmosphere exchanges of ammonia (NH₃), mainly due to limitations in measurement techniques. In this study, the eddy covariance (EC) technique based on an open-path quantum cascade laser (QCL) spectrometer was used to measure the NH₃ fluxes at a typical cropland in the North China Plain, one of the global NH₃ hotspots. It is the first attempt of measuring both NH₃ volatilization and deposition fluxes at an agricultural ecosystem using the open-path instrument-based EC technique. During the one-month experimental period, the NH₃ fluxes were characterized by enhanced emissions after fertilizer application and persistent dry depositions after ploughing practice, with the flux magnitude varying from −0.293 to 7.29 (median: −0.042) mg N m⁻² h⁻¹. Nearly 93% of the half-hourly fluxes (absolute values) exceeded the mean instrumental flux detection limit of 9.6 μg N m⁻² h⁻¹. Nitrogen loss rate from the wheat field through NH₃ volatilization was 0.57–0.71% relative to the applied nitrogen fertilizers. Ammonia deposition dominated the period after the ploughing practice, showing an average deposition rate of 0.014 kg N ha⁻¹ d⁻¹ with a significant diurnal pattern. Both the local emission sources and meteorological conditions influenced the variation of NH₃ dry deposition. The deposition fluxes measured by the EC technique were nearly one third the results modelled by the widely used inferential model method, but the difference needs to be validated by more observations that includes different surface and meteorological conditions. This study suggests that this open-path QCL-based EC instrument is an effective tool for long-term and high-frequency measurements of ecosystem NH₃ exchanges. It also enables cross-validation between different methods to improve the understanding in the atmospheric reactive nitrogen cycling.

* Corresponding author.

E-mail address: liu310@cau.edu.cn (X. Liu).

¹ These authors contributed equally to this work.

1. Introduction

Ammonia (NH_3) is the most important alkaline gas in the atmosphere. Agricultural activities, particularly NH_3 volatilization following synthetic fertilizer application, is one of the major sources of anthropogenic NH_3 emissions (Bouwman et al., 1997), and also an important pathway of cropland nutrient loss (Sha et al., 2021; Zhu, 1997). A substantial part of the emitted NH_3 turns back to the land surface through dry deposition of gaseous NH_3 and particulate ammonium, and wet deposition of ammonium (Asman et al., 1998). These nitrogen (N) loads benefit the ecosystems as nutrient input for primary production, but also cause a lot of environmental and public health problems, such as biodiversity loss, eutrophication and haze pollution (Liu et al., 2011; Wen et al., 2021). Hence, accurate quantification of NH_3 volatilization and deposition fluxes, particularly at the agricultural regions, is essential for the understanding of local and regional N budget. However, large uncertainties and challenges still remain in the *in-situ* measurements of NH_3 fluxes, mainly due to the intrinsic nature of NH_3 , e.g., strong stickiness and high reactivity.

So far, the eddy covariance (EC) technique, which based on simultaneous measurements of turbulent air movements and gas concentrations above the ground, is the most direct approach to measure the energy and mass exchanges (turbulent fluxes) between ecosystems and the atmosphere (Aubinet et al., 2000). For NH_3 flux measurement, EC has advantages over other methods, such as the dynamic chamber method (e.g., Li et al., 2015), the mass balance method (e.g., Cai et al., 2002), the aerodynamic gradient method (e.g., Milford et al., 2009) and the inferential model method (e.g., Tang et al., 2009), because it can directly quantify both NH_3 emission and deposition fluxes, and also produce temporally continuous data that represent the spatial averages at the field scale (Ferrara et al., 2016; Sintermann et al., 2011). In the past, however, the application of EC is seriously limited by the lack of fast-response (≥ 10 Hz) and highly sensitive NH_3 analyzers, particularly such analyzers that can be driven by solar batteries in the field (Pan et al., 2021; Sun et al., 2015). Recently, a portable and solar-powered open-path NH_3 analyzer (HT8700, HealthyPhoton Co., Ltd., Ningbo, China) based on quantum cascade laser (QCL) spectrometer has become available. It is the first commercial open-path instrument especially designed for EC flux measurements of NH_3 . According to laboratory and field tests, this instrument was proven to be an effective tool to measure NH_3 fluxes under a wide range of environmental conditions (Wang et al., 2021).

In this study, we used this new instrument and conducted EC flux measurements of NH_3 at a typical agricultural site in the North China Plain, one of the global NH_3 hotspots (Pan et al., 2018; Van Damme et al., 2018). The experiment was done on a cropland during the wheat season and lasted for five weeks. Although Wang et al. (2021) had tested this new instrument and made the first attempt of EC flux measurement at a cropland (rice paddy), their study only aimed to evaluate the instrumental performance based on one-week measurements of NH_3 volatilization flux after applying a little amount of N fertilizers on the bare soil during the fallow season. So, this is the first attempt of measuring both NH_3 volatilization and deposition fluxes at an agricultural ecosystem using the open-path instrument-based EC technique. The main purpose of this study is to investigate the characteristics of the NH_3 fluxes at this agricultural site during the autumn month, and quantify the NH_3 dry deposition to the cropland and the nitrogen loss through NH_3 volatilization. Since the open-path QCL offered half-hourly NH_3 concentration data, we also modelled the dry deposition of NH_3 using a widely adopted inferential model with an empirical parameterization scheme, to test the model performance in this specific case study.

2. Methodology

2.1. Site description

The field experiment was conducted at a winter-wheat and summer-maize rotation field ($36^\circ 51' 42.46''\text{N}$, $115^\circ 01' 46.66''\text{E}$, 37 m a.s.l.) near the Quzhou experimental station of China Agricultural University. The site is subject to a temperate continental monsoon climate, with an annual mean air temperature of 13.9°C and annual precipitation of 517 mm (Xu et al., 2015). The field soil is classified as salinized Camisol, a calcareous sandy loam with a pH in the surface layer (0–10 cm) of 8.3. Wheat season usually begins in mid-October and ends in early June. Fertilizers are broadcast as basal dressing before sowing, immediately followed by ploughing, and in the form of topdressing in the spring. In this study, the EC measurement was conducted during the wheat season (October 12 to November 16, 2020). The satellite map of the experimental field, collected during the previous wheat season, though, shows the location of the EC mast and the surrounding field plots (Fig. 1a). However, field operations of these plots were different in terms of fertilizer application, ploughing and irrigation, as well as the type and amount of the applied fertilizers (Table 1).

2.2. Eddy covariance measurements

The NH_3 fluxes were measured using an EC system consisted of the HT8700 open-path NH_3 analyzer, a three-dimensional sonic anemometer [CSAT-3A, Campbell Scientific Inc. (CSI), Logan, USA], an open-path gas analyzer (EC150, CSI, Logan, USA) for carbon dioxide (CO_2) and water vapor (H_2O) detection, and a measurement and control datalogger (CR6, CSI, Logan, USA). Raw data of the wind velocities and gas densities were saved in the datalogger at a frequency of 10 Hz. As shown in Fig. 1b, the sonic anemometer and the $\text{CO}_2/\text{H}_2\text{O}$ analyzer were both amounted at a height of 1.75 m. Vertical installation was adopted for the NH_3 analyzer, with its optical path center being 1.78 m above the ground and 0.35 m away from the anemometer center. The EC system had a total power consumption of about 50 W at normal conditions. It was fully powered by solar batteries during the whole measurement period. The analyzer's optical cell mirrors were manually cleaned once the optical signal strength decreased to 30–40% (Wang et al., 2021). An air temperature and moisture probe (HMP155A, Vaisala Corporation, Vantaa, Finland) was used to record the air temperature and relative humidity. Hourly precipitation was observed by a microclimate station 2 km away from the experimental field.

2.3. Processing of eddy covariance data

2.3.1. Flux calculation and correction

Ammonia fluxes were calculated as the covariance of the vertical wind velocity and the NH_3 density over the time interval of 30 min. The data processing procedures followed the method described in Wang et al. (2021), including de-spiking of raw data, double rotation of wind components, lag time correction between vertical wind velocity and NH_3 concentration, and detrending. An autoregressive running mean filter (McMillen, 1988) with a time constant of 150 s was applied on the NH_3 time series to remove the low-frequency trend in the NH_3 signal. The raw half-hourly fluxes were corrected for the spectral attenuation at the low- and high-frequencies, according to the analytical methods proposed by Moncrieff et al. (1997, 2004). Variation in water vapor, temperature and pressure affect the NH_3 flux measurements by means of the WPL effect (Webb et al., 1980) and the spectroscopic effect (Burba et al., 2019). The former is caused by water vapor dilution on the NH_3 density and by thermal expansion and contraction of the air parcel due to temperature fluctuation. The latter is related to changes in the spectroscopic properties of NH_3 absorption line due to variations in the above environmental variables. These effects were corrected followed the method in Wang et al. (2021), originally proposed by McDermitt

et al. (2011); sensible heat flux, water vapor density and water vapor flux that required for these corrections were derived from the data measured by the EC system. The surface-heating effect of open-path gas analyzers (Burba et al., 2008) was assumed to be negligible, as the HT8700 was vertically installed, with the heat source being in the above position. All the above steps, except the WPL and spectroscopic corrections, were implemented using the EddyPro software package (version 6.2.0, LI-COR Biosciences, Lincoln, USA).

2.3.2. Flux footprint analysis

The overall footprint during the NH_3 emission period (October 14–17, 2020) were analyzed using the model proposed by Kljun et al. (2015). The model code is online available at <http://footprint.kljun.net>, which can be used to produce 2-dimensional plot that aggregates all half-hourly footprints over a time period. The input data of the model includes measurement height, roughness length, wind speed, wind direction, boundary layer height, Monin-Obukhov length, friction velocity, and standard deviation of lateral wind velocity fluctuations. The roughness length was prescribed at 0.003 m, as the field surface was flat and covered with a few straws of maize (Stull, 1988). The boundary layer height was parameterized according to Kljun et al. (2015). Other input variables were derived from the sonic anemometer data.

As shown in Fig. 1a, at least 85% of the NH_3 emissions were contributed by the field plots 1–4 (hereafter referred to as the target area), which had the same timing of fertilization and ploughing practices (Table 1). However, around the target area the field operations were quite different. For example, in the west (field plot 5) and east, fertilization and ploughing were conducted before October 10; in the north and south were residential houses and orchards (brown area in Fig. 1a), which did not receive fertilizers during the experimental period. It implies negligible NH_3 emissions in the above areas, which would bias the calculation of the true fluxes from the target area. So, the measured half-hourly fluxes were corrected following Eqs. (1) and (2).

$$F_m = k_1 F_1 + k_2 F_2 \quad (1)$$

$$k_1 + k_2 = 1 \quad (2)$$

Here, F_m is the measured EC flux; k_1 and k_2 represent the footprint fractions of the target area and its surrounding area as a whole, respectively; F_1 is the corrected flux that could represent the true NH_3 flux (from the target area) caused by fertilizer application; F_2 is the flux of the surrounding areas, which is assumed to be zero. k_1 was calculated using the footprint tool proposed by Neftel et al. (2008), which is based on the analytical model by Kormann and Meixner (2001). This tool is specifically used to estimate the footprint fraction of a given

quadrangular surface area defined by the user. The input data is similar as the Kljun model; x and y coordinates of the EC instruments and the quadrangular area are also needed. This tool is implemented in an EXCEL® spreadsheet in order to facilitate data input and handling. It can be downloaded at <https://zenodo.org/record/816236>.

2.3.3. Quality control and gap-filling

Quality control of the NH_3 fluxes was done as follow. First, fluxes were filtered if the optical signal strength of the NH_3 analyzer was below 40% (Wang et al., 2021). Second, fluxes were rejected if a quality flag of 2 was assigned according to the stationarity and integral turbulence tests proposed by Mauder and Foken (2015). Third, a friction velocity threshold of 0.05 m s^{-1} was adopted (Gu et al., 2005) to filter nighttime NH_3 fluxes. Finally, spikes in the flux data were removed if exceeding two times the standard deviation of the adjacent six flux values. Data gaps were filled to calculate the cumulative flux. Linear interpolation was applied for the NH_3 emission period, and the mean diurnal variation (MDV) method (Falge et al., 2001) was used for the deposition period.

2.3.4. Random error and flux detection limit

Total random error of each half-hourly flux is estimated according to Finkelstein and Sims (2001). The random error component caused by instrumental noise, also regarded as the flux detection limit (F_{det}), i.e., the lowest flux that the instruments can measure, is estimated using the method described by Wang et al. (2021). To calculate F_{det} , the instrumental noise of the HT8700 analyzer is needed; it is estimated used the Allan variance method (Werle et al., 1993) by analyzing each half-hourly data collected during the experiment. As suggested by Rannik et al. (2016), only NH_3 data with signal-to-noise ratio less than 3 were selected for this calculation.

2.4. Modelling of ammonia dry deposition

Ammonia dry deposition fluxes (F_d) were estimated using the commonly adopted inferential method from October 18 to November 14, 2020. In this method, the measured NH_3 concentration (C_z) is paired with a modelled dry deposition velocity (V_d) to calculate the flux (Zhu et al., 2021).

$$F_d = -C_z V_d \quad (3)$$

$$V_d = (R_a + R_b + R_c)^{-1} \quad (4)$$

$$R_a(z) = (ku^*) \left[\ln \left(\frac{z-d}{z_0} \right) - \varphi_h \left(\frac{z-d}{L} \right) + \varphi_h \left(\frac{z_0}{L} \right) \right] \quad (5)$$

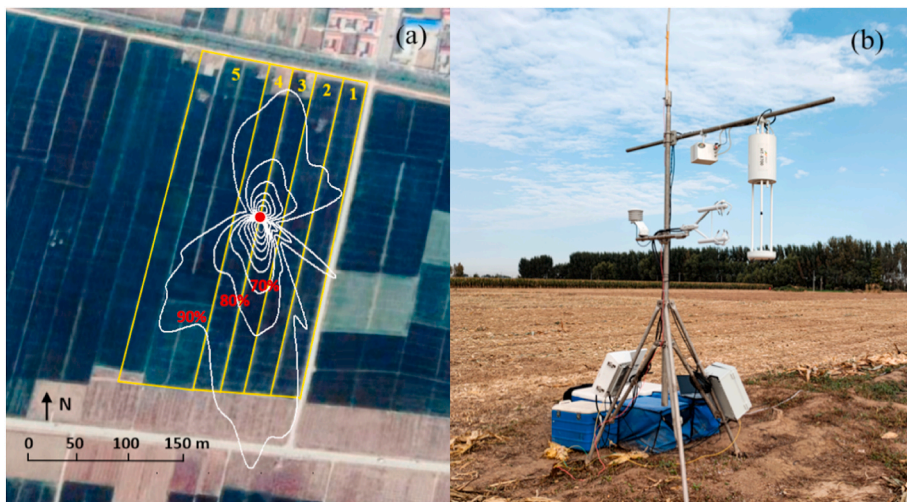


Fig. 1. (a) Layout of the experimental field and (b) a picture of the eddy covariance (EC) system during the measurement period (October 12, 2020). The background map is the Google Earth satellite image on March 20, 2020. The red dot shows the location of the EC system. The areas enclosed by yellow lines indicate the experimental field plots. The aggregated footprint during the ammonia emission period (October 14–17, 2020) is shown with white contour lines from 10% to 90% in steps of 10%. (For interpretation of the references to colour in this figure legend, the reader is referred to the Web version of this article.)

$$R_b = (2 / ku^*) (S_c / P_r)^{2/3} \quad (6)$$

$$R_c = (1 / R_{gs})^{-1} \quad (7)$$

Here, V_d is calculated based on a big-leaf resistance analogy model, with R_{a} , R_b and R_c representing the aerodynamic resistance, boundary layer resistance, and surface or canopy resistance, respectively; z is the sensor height; k is the von Karman constant; d is the zero-plane displacement height; z_0 is the roughness length; ψ_h is the integrated stability functions for entrained scalars; u^* and L are the friction velocity and Monin-Obukhov length, respectively; P_r is the Prandtl number; S_c is the Schmidt number; R_{gs} is the surface bulk resistance component for the soil, leaf litter, etc., at the ground surface. More detailed information about the above parameters can be found in Wesely and Hicks (1977), Wesely (1989) and Erisman et al. (1994). In this study, the field surface is always considered as bare soil, because the wheat seedlings came out in the late October, and the aboveground biomass was assumed to be negligible even at the end of the experimental period. So, R_c is calculated with its simplified form by omitting the resistance components related to canopy. The soil volumetric moisture was treated as a constant (18%) due to lack of measurement data. This inferential model with the above empirical parameterization scheme is quite practical in use and has been employed in many studies (e.g., Kuang et al., 2016; Zhu et al., 2021). The model performance was tested in this specific case study by comparing the modelled deposition fluxes with the EC fluxes.

3. Results and discussion

3.1. Data availability and instrument performance

In total, we obtained 1019 half-hourly NH_3 concentration data, corresponding to a data coverage of 74%, if excluding the continuous data gap from October 27 to November 3 due to malfunction of data-logger. Nearly 70% of the missing data were caused by raindrop or dew on the optical mirrors, while the others by environment dust or particle, which all led to laser signal attenuation. After applying quality control, data availability of the NH_3 flux was 50%; about 48% of the rejected flux data were the result of attenuated laser signal, and 52% were due to other quality control criteria.

The instrumental noise (1σ) of the NH_3 analyzer was estimated at $0.41 \pm 0.06 \text{ nmol mol}^{-1}$ (ppbv) at 10-Hz sampling frequency, being larger than the estimate (0.30 ± 0.05 ppbv) reported by Wang et al. (2021). Accordingly, the flux detection limit of the EC system averaged at $9.6 \pm 1.5 \mu\text{g N m}^{-2} \text{ h}^{-1}$ (95% confidence interval). Nearly 93% of the half-hourly fluxes (absolute values) exceeded this mean detection limit. The total flux random error showed a mean value of 13% relative to the flux magnitude. The NH_3 analyzer was calibrated before the field campaign following the method described by Wang et al. (2021). According to previous laboratory tests (Wang et al., 2021), after calibration the NH_3 analyzer reported a concentration difference of less than 10% as compared to two commercially available high-sensitivity closed-path NH_3 analyzers (model G2103 of Picarro and model EAA-911 of Los Gatos Research), implying that its measurement accuracy is efficient for

field deployment.

3.2. Variation of ammonia concentrations and fluxes

Fig. 2b shows the temporal variation of the half-hourly NH_3 concentrations during the experimental period. It varied between 1.7 and 40.7 ppbv, with a mean value of 20.8 ± 5.1 ppbv ($27.4 \pm 6.7 \mu\text{g m}^{-3}$). The mean value is lower than the annual estimates ($40.3 \pm 3.3 \mu\text{g m}^{-3}$) reported by a recent study (Feng et al., 2022), in which the atmospheric NH_3 concentration was measured at nine sites across Quzhou County from 2018 to 2019. Despite the difference between their and our results, likely due to seasonal and spatial variability, both the two studies show much higher concentration than those observed in East Asia, Europe, the United State and other areas in China (see Table S4 in Feng et al., 2022). Feng et al. (2022) concludes that the high-level NH_3 concentration is related to the intensive local emissions from both agricultural sources (fertilizer application and concentrated livestock production) and non-agricultural sources (fossil fuel, waste and biomass burning); the two emission sectors almost contributed the same percentages in both rural and urban areas in Quzhou County. Normally, these emitted NH_3 has an atmospheric lifetime of a few hours to 5 days, which could be transported over regional scale distances and affect the local NH_3 abundance (Aneja et al., 2001).

The largest concentration peak appeared in the afternoon of October 13, right after the fertilizer application. However, the rainfall occurred during the nighttime, which lasted until the morning of the following day, contaminated the collected data. After cleaning the optical mirrors, another peak was observed until October 16, most likely related to the enhanced NH_3 volatilization. Thereafter, the concentration varied following a typical diurnal pattern as shown in Fig. 3c, with the diurnal peak occurring at 08:00–08:30 local standard time. Similar morning peak was also found in many other studies (Gu et al., 2022; He et al., 2020; Wentworth et al., 2016). The peak was likely caused by the dew evaporation due to increased air temperature and the downward mixing of NH_3 from the residual layer due to the developing turbulence after sunrise.

The NH_3 fluxes was characterized by enhanced emissions after fertilization and persistent depositions following the ploughing practice, with an exception in the daytime of November 15, during which positive NH_3 fluxes were clearly observed (Fig. 2b–d). The minimum, maximum, mean and median values of the fluxes were -0.293 , 7.29 , 0.106 and $-0.042 \text{ mg N m}^{-2} \text{ h}^{-1}$, respectively. As planned, ploughing and sowing are implemented on the next day following fertilization. However, it was delayed by three days due to a rainfall soon arrived after fertilization. The rain helped to dissolve the fertilizer granules, but neither the rain amount (9.7 mm in total) nor the rain intensity was large enough to dissolve granular fertilizers (ammonium-based) and bring them to deeper soil. A large part of the fertilizers stayed on the surface soil after the rain, which increased the potential of ammonium conversion to gaseous NH_3 during the daytime. As a result, considerable NH_3 emissions were observed on October 14 and 15, which showed a strong correlation ($p < 0.01$) with the air temperature (Fig. 2a and b). However, on October 16 and 17, the emission fluxes dropped by 1–2 orders of

Table 1
Field operations of the experimental field.

Plot	Date of field operations			Fertilization rate (kg N ha^{-1})		
	Fertilization	Ploughing	Irrigation	Fertilizer 1 ^a	Fertilizer 2 ^b	Total
1	October 13	October 17	November 16	120	0	120
2	October 13	October 17	November 15	96	0	96
3	October 13	October 17	November 14	76.8	22.6	99.4
4	October 13	October 17	November 14	57.6	45.1	102.7
5	October 6	October 10	November 10–11	120	0	120

^a Granular chemical compound fertilizer with nitrogen (N), phosphorus (P) and potassium (K) contents of 16%, 17% and 10%, respectively.

^b Granular organic fertilizer with N, P and K contents of 0.94%, 1.76% and 1.96%, respectively.

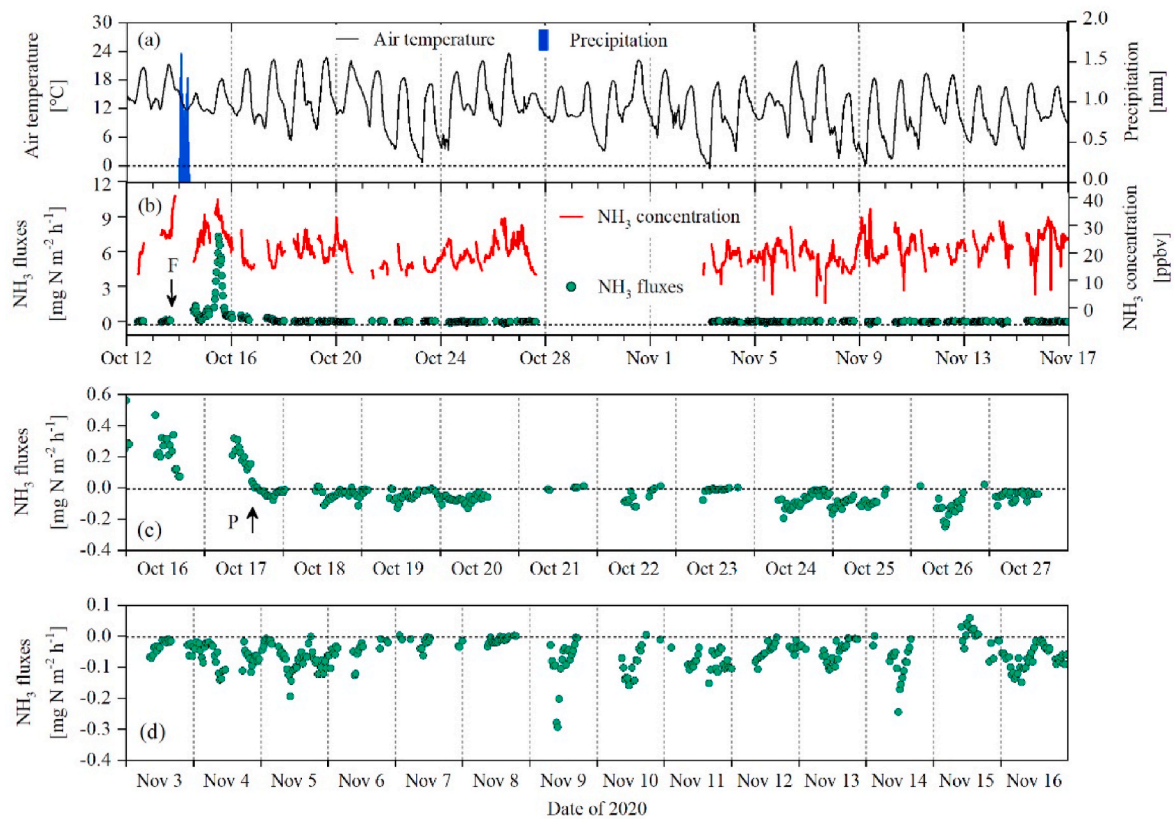


Fig. 2. Temporal variability of the (a) hourly air temperature and precipitation, and (b–d) half-hourly ammonia (NH_3) concentration and fluxes. Flux data in panels c and d (October 16 to November 16, 2020) are the same as those in panel b, presented with smaller range of y axis for the purpose of clearer inspection. Arrows with a letter of “F” and “P” indicate the time of fertilizer application and ploughing, respectively.

magnitude, probably because most soil ammonium had been consumed by the processes of soil nitrification and NH_3 volatilization in the previous days. After the ploughing practice (depth: 25 cm), the experimental field immediately turned to a net sink of NH_3 towards the end of the experiment. Unexpectedly, we observed continuous positive NH_3 fluxes from 11:30 to 15:30 on November 15. According to the footprint analysis by the Kljun model, nearly 90% of the emission sources located in the field plots 3, 4 and 5, where flood irrigation had just been implemented during the previous days. We guess that these emission signals were caused by unknown sources beyond the experimental fields, which were not well investigated during the experimental period.

Ammonia fluxes from October 14 to 17 were corrected due to spatial heterogeneity of NH_3 emissions (Eqs. (1) and (2)). According to the footprint analysis by the Nefel model, the mean total footprint fraction of the field plots 1–4 was $88\% \pm 10\%$, which means that the emission fluxes would increase by 14% on average after this correction. The above fraction (mean: 88%) agrees well with that calculated by the Kljun model (Fig. 1a). The Kljun and Nefel footprint models are used for different purposes in this study. Although their parameterization schemes are not fully the same, they report almost the same results in this study, not only for aggregated flux over a time period, but also for half-hourly flux (data not shown). This is because the two model have similar performance for the cases with flat and homogeneous surface and EC sensors being close to the ground (Kormann and Meixner, 2001; Kljun et al., 2015).

A clear diurnal pattern of the deposition flux was observed (Fig. 3a). It had a positive correlation with the air temperature, despite a lag of about 3 h (Fig. 3d). Both the deposition rate and the wind speed were larger during the daytime; both of them had an inflexion point at 18:00 (Fig. 3a and e). Usually, dry deposition of NH_3 is influenced by the local emission sources and the air transport, which both dependent on the

meteorological conditions (Asman et al., 1998). Higher temperature and wind speed means more NH_3 emissions from the sources. Meanwhile, temperature and wind speed could be the indicators of thermal and mechanical turbulence strength, respectively, which are both closely related to NH_3 diffusion and transport. Fig. 4a shows that most wind was coming from the southern directions during the deposition period. We also observed differences in the deposition rates categorized by wind direction; all bin-averaged values were lower than $0.05 \text{ mg N m}^{-2} \text{ h}^{-1}$, except those of the direction sector of $180\text{--}240^\circ$ (Fig. 4b). In this direction, approximately 10 km away from the experimental site, it is the center of the Quzhou county. Higher deposition from that direction sector was likely caused by other anthropogenic NH_3 sources in the county center.

3.3. Nitrogen loss due to ammonia volatilization

Fertilizer application led to significant NH_3 emissions from October 14 to 17, so the N fertilizer loss due to NH_3 volatilization was estimated. However, there are three uncertainties.

First, the cumulative emission from October 14 to 17 amounted to $0.642 \text{ kg N ha}^{-1}$. Since the EC fluxes represent the net NH_3 exchanges, the above estimate is the result of the total volatilization offset by the dry deposition. The latter was roughly estimated at $0.044 \text{ kg N ha}^{-1}$ from October 14 to 17, assuming that the deposition intensity during this period was the same to that after the ploughing practice (see Section 3.4). As a result, the total NH_3 volatilization flux was estimated at $0.686 \text{ kg N ha}^{-1}$. Second, NH_3 emissions during the rainfall were not included in the calculation due to lack of supportive data. Third, even in the target area, the amounts and type of the applied fertilizers differed from plot to plot (Table 1). We ignore the potential influence arise from this uncertainty, and divide the total volatilization by the fertilization rate range

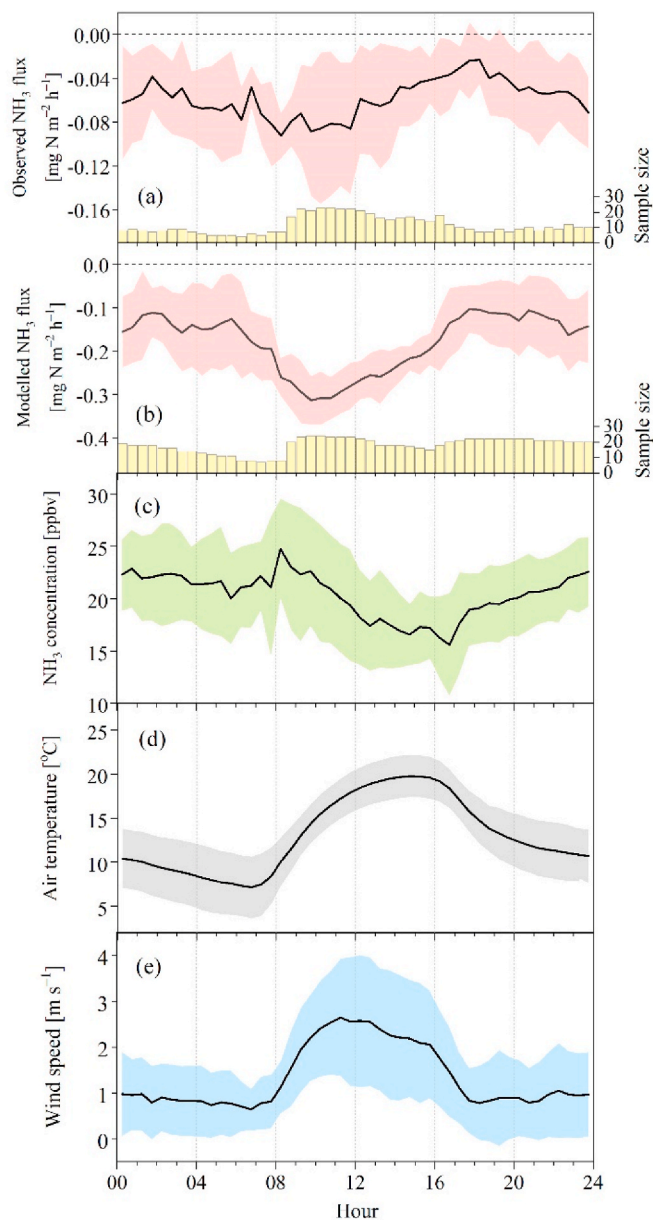


Fig. 3. Mean diurnal variations of the (a) observed ammonia (NH_3) deposition fluxes, (b) modelled NH_3 deposition fluxes, (c) NH_3 concentration, (d) air temperature, and (e) wind speed during the period of October 18 to November 16, 2020. The shaded areas show the standard deviation of each variable. The histogram in panels a and b shows the sample sizes of the NH_3 flux of each half-hour period.

(96–120 kg N ha^{-1}) within the target area.

As a result, the N fertilizer loss rate due to NH_3 volatilization was estimated at 0.57–0.71%. It is much lower than the results ($9.3 \pm 6.2\%$) reported by previous studies that conducted on wheat fields in the North China Plain using the micrometeorological methods (Huo et al., 2015; Pacholski et al., 2006; Yang et al., 2014). First, the lower estimate can be explained, to a large part, by the rainfall right after fertilizer application. With moderate rain intensity (9.7 mm), the rainwater accelerated the dissolution of fertilizer and the process of soil nitrification, which reduced the availability of soil ammonium. Meanwhile, the data gap during the rainfall (18:00 of October 13 to 10:00 of October 14) may cause significant underestimation in the total volatilization, but the amount is difficult to quantify due to lack of supportive data. Second, the surface soil (0–25 cm) was ploughed four days after fertilization, which

also decreased the NH_3 emissions quickly (Fig. 2c). Third, the use of compound fertilizer and organic fertilizer is also another reason accounting for the low emission rate, which has lower emission potential as compared to other N fertilizers, e.g., ammonium bicarbonate and urea (Lian et al., 2018; Sha et al., 2021).

3.4. Dry deposition of ammonia

The wheat field acted as a persistent sink of NH_3 during most time of the experimental period, showing an average deposition flux of $0.061 \text{ mg N m}^{-2} \text{ h}^{-1}$ after the ploughing practice. The diurnal pattern was quite different from some studies carried out at natural ecosystems using the EC technique (Pan et al., 2021; Zöll et al., 2016). In these studies, biological emissions, e.g., through leaf drying and stomatal release, play an important role in the NH_3 exchanges, so that bi-directional fluxes were observed, and the ecosystems could sometimes turn into net source of NH_3 at noon. By contrast, in this study, deposition from the local emission sources controlled the net exchange diurnal variation most of the time. After filling the data gaps with the MDV method, we got an average daily deposition of $0.014 \text{ kg N ha}^{-1} \text{ d}^{-1}$ from October 18 to November 16, 2020, and thus a rough annual estimate of $5.11 \text{ kg N ha}^{-1} \text{ a}^{-1}$ by assuming the same deposition rate throughout the year. Given the good performance of the EC system, longer observations are expected to constrain the annual dry deposition of this agricultural region.

The inferential model method is the most common method for the quantification of site-scale reactive nitrogen deposition (Clarke et al., 1997). Using this method, Xu et al. (2015) estimated the monthly dry deposition of NH_3 at the Quzhou experimental station, which is very close to our experimental field (2 km in the northwest). They reported an average annual deposition rate of $10.5 \text{ kg N ha}^{-1} \text{ a}^{-1}$ from 2010 to 2014, which is nearly twice as our estimate. Despite different studied periods, depositions calculated by the two studies are comparable if taking the following uncertainties into account. First, dry deposition of NH_3 in this region has significant seasonal pattern, and deposition in October and November is the weakest of the year (e.g., Pan et al., 2012). Second, recent studies indicated that the anthropogenic NH_3 emission of China has peaked around 2010 and started to fall thereafter (e.g., Liu et al., 2020), so this national-wide trend could also apply to the local emission strength in this region and affect the inter-annual variation of NH_3 dry deposition.

Deposition fluxes of NH_3 was modelled using the inferential method at a timestamp of half-hour. The model captures the variability of the deposition, and reproduces the same diurnal pattern as the observed (Fig. 3a and b). The estimated NH_3 deposition velocity (V_d) averaged to $0.42 \pm 0.22 \text{ cm s}^{-1}$, which is in the range of those reported by previous studies in the North China Plain (Shen et al., 2009; Pan et al., 2012; Xu et al., 2015). The aerodynamic and boundary layer resistances determined the variation and magnitude of V_d and thus the deposition flux, because both R_a and R_b had significant diurnal patterns, with much smaller values than R_c in the daytime, during which the major deposition occurred. By contrast, R_c had less contribution to V_d , because the surface was treated as bare soil and therefore many canopy processes that affecting the deposition pathway are ignored (Wesely, 1989; Zhang et al., 2002). Fig. 5a shows that the inferential model gives much larger deposition rates than the observed, nearly by a factor of two according to the linear regression analysis. The results of the comparison are similar using the half-hourly daytime and nighttime data alone, respectively (Fig. 5b and c). The large discrepancy suggests uncertainties in both methods. One potential uncertainty associated with the EC fluxes is the overestimation of nighttime data due to rejection of low turbulence data. But elimination of this bias would even increase the discrepancy. So, it is possible that the simplified parameterization of the NH_3 deposition velocity, the surface resistance in particular, may have large uncertainty in modelling the deposition fluxes in this specific case. However, more observations are needed to validate this discrepancy. With this new open-path instrument, it is also expected in the future to

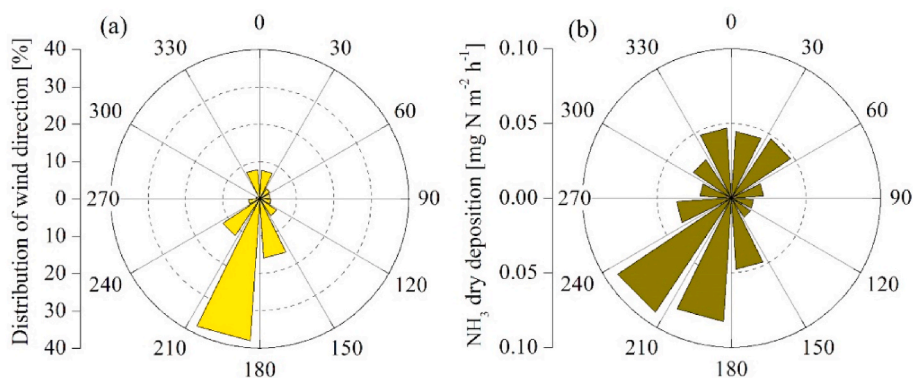


Fig. 4. (a) Distribution of the wind direction, and (b) average ammonia (NH_3) dry deposition rates categorized by wind direction from October 18 to November 14, 2020.

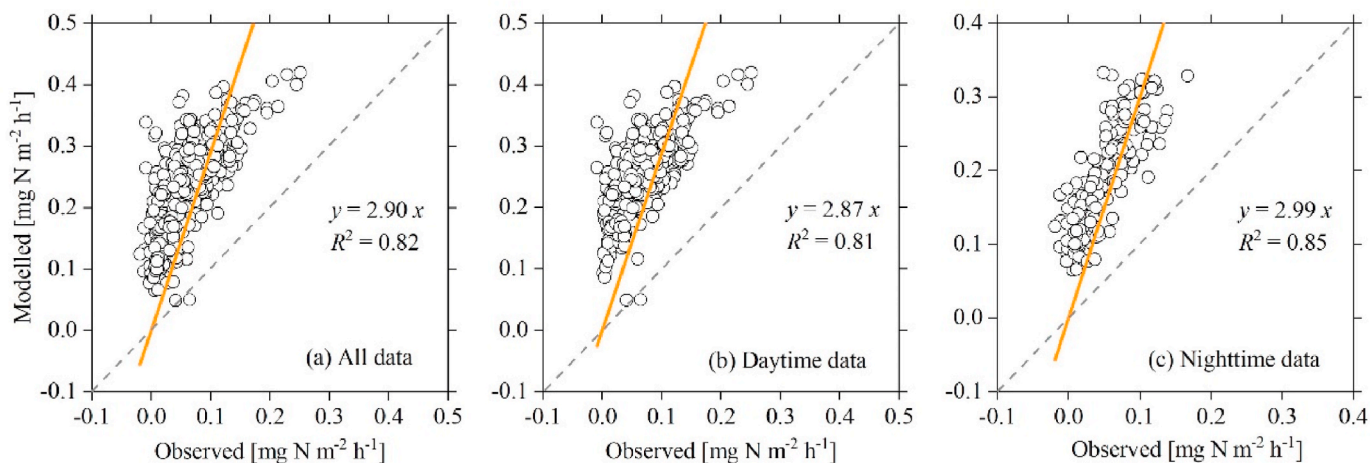


Fig. 5. Comparison of the observed and modelled half-hourly ammonia deposition rates (negative values of the deposition fluxes). The orange lines indicate the linear regression with zero-intercept. The black dashed lines mark the $y = x$ line. Flux data from October 18 to November 14, 2020, are selected for the comparison. (For interpretation of the references to colour in this figure legend, the reader is referred to the Web version of this article.)

investigate the deposition characteristic during the growing season with vegetation, and to cross-validate with the more complicated bi-directional resistance models (e.g., Nemitz et al., 2000) in this high-deposition agricultural region.

4. Conclusions

An open-path quantum cascade laser-based eddy covariance instrument succeeded to measure both NH_3 volatilization and dry deposition fluxes at a typical cropland in the North China Plain during the autumn month. The cumulative nitrogen loss through NH_3 volatilization from the wheat field was found small (0.57–0.71%) relative to the applied nitrogen fertilizers. Ammonia emissions were largely suppressed by the rainfall following the fertilization and the ploughing practice implemented a few days later. Deposition fluxes of NH_3 dominated the experimental period following the ploughing practice, showing a significant diurnal pattern, which was controlled by both the local emission sources and the meteorological conditions. The average deposition rate was $0.014 \text{ kg N ha}^{-1} \text{ d}^{-1}$, which was nearly half the result estimated by the inferential model method at a nearby experimental site from 2010 to 2014. The difference can be explained by the seasonal and inter-annual variation of the NH_3 dry deposition in this region. However, even larger difference was found according to the direct comparison between the observed deposition and those modelled by the inferential method using the on-site meteorological data. But the difference still needs to be validated by more observations that includes different surface and

meteorological conditions. This study suggests that this open-path QCL-based EC instrument is an effective tool for long-term and high-frequency measurements of ecosystem NH_3 exchanges. It also enables cross-validation between different methods to improve the understanding in the atmospheric reactive nitrogen cycling.

CRediT authorship contribution statement

Kai Wang: Methodology, Writing – original draft, Validation. **Jingxia Wang:** Investigation, Formal analysis, Visualization. **Zhichen Qu:** Investigation. **Wen Xu:** Writing – review & editing. **Kai Wang:** Writing – review & editing. **Hongyan Zhang:** Resources. **Jianlin Shen:** Software. **Peng Kang:** Investigation. **Xiaojie Zhen:** Resources. **Yin Wang:** Writing – review & editing. **Xunhua Zheng:** Writing – review & editing, Validation. **Xuejun Liu:** Conceptualization, Funding acquisition, Supervision.

Declaration of competing interest

The authors declare that they have no known competing financial interests or personal relationships that could have appeared to influence the work reported in this paper.

Acknowledgements

This work was financially supported by the National Research

Program for Key Issues in Air Pollution Control (grant number DQGG0208), the National Basic Research Program of China (grant numbers 2018YFC0213301, 2017YFD0200101), the National Natural Science Foundation of China (grant numbers 41975169, 42175137), the Chinese Academy of Sciences (grant number ZDBS-LY-DQC007) and the High-level Team Project of China Agricultural University. The authors also thank Mr. Mengmeng Liu from HealthyPhoton Co., Ltd. for the technical assistance in the field experiments.

References

- Aneja, V.P., Roelle, P.A., Murray, G.C., Southerland, J., Erisman, J.W., Fowler, D., Asman, W.A.H., Patni, N., 2001. Atmospheric nitrogen compounds: II. Emissions, transport, transformation, deposition, and assessment. *Atmos. Environ.* 35, 1903–1911.
- Asman, W.A.H., Sutton, M.A., Schjørring, J.K., 1998. Ammonia: emission, atmospheric transport and deposition. *New Phytol.* 139, 27–48.
- Aubinet, M., Grelle, A., Ibrom, A., Rannik, Ü., Moncrieff, J., Foken, T., Kowalski, A.S., Martin, P.H., Bernbigler, P., Bernhofer, C., Clement, R., Elbers, J., Granier, A., Grunwald, T., Morgenstern, K., Pilegaard, K., Rebmann, C., Snijders, W., Valentini, R., Vesala, T., 2000. Estimates of the annual net carbon and water exchange of forests: the EUROFLUX methodology. *Adv. Ecol. Res.* 30, 113–175.
- Bouwman, A.F., Lee, D.S., Asman, W.A.H., Dentener, F.J., Van Der Hoek, K.W., Olivier, J.G.J., 1997. A global high-resolution emission inventory for ammonia. *Global Biogeochem. Cycles* 11, 561–587.
- Burba, G.G., Anderson, T., Komissarov, A., 2019. Accounting for spectroscopic effects in laser-based open-path eddy covariance flux measurements. *Global Change Biol.* 24, 2189–2202.
- Burba, G.G., Mcdermitt, D.K., Grelle, A., Anderson, D.J., Xu, L., 2008. Addressing the influence of instrument surface heat exchange on the measurements of CO₂ flux from open-path gas analyzers. *Global Change Biol.* 14, 1854–1876.
- Cai, G., Chen, D., Ding, H., Pacholski, A., Fan, X., Zhu, Z., 2002. Nitrogen losses from fertilizers applied to maize, wheat and rice in the North China Plain. *Nutrient Cycl. Agroecosyst.* 63, 187–195.
- Clarke, J.F., Edgerton, E.S., Martin, B.E., 1997. Dry deposition calculations for the clean air status and trends network. *Atmos. Environ.* 31, 3667–3678.
- Erisman, J.W., Van Pul, A., Wyers, G.P., 1994. Parameterization of surface resistance for the quantification of atmospheric deposition of acidifying pollutants and ozone. *Atmos. Environ.* 28, 2595–2607.
- Falge, E., Baldocchi, D., Olson, R.J., Anthoni, P., Aubinet, M., Bernhofer, C., Burba, G., Ceulemans, R., Clement, R., Dolman, H., Granier, A., Gross, P., Grünwald, T., Hollinger, D., Jensen, N.-O., Katul, G., Kerönen, P., Kowalski, A., Ta Lai, C., Law, B. E., Meyers, T., Moncrieff, J., Moors, E., Munger, J.W., Pilegaard, K., Rannik, Ü., Rebmann, C., Suyker, A., Tenhunen, J., Tu, K., Verma, S., Vesala, T., Wilson, K., Wofsy, S., 2001. Gap filling strategies for defensible annual sums of net ecosystem exchange. *Agric. For. Meteorol.* 107, 43–69.
- Feng, S., Xu, W., Cheng, M., Ma, Y., Wu, L., Kang, J., Wang, K., Tang, A., Collett, J.L., Fang, Y., Goulding, K., Liu, X., Zhang, F., 2022. Overlooked nonagricultural and wintertime agricultural NH₃ emissions in Quzhou County, North China Plain: evidence from 15N-stable isotopes. *Environ. Sci. Technol. Lett.* 9 (2), 127–133.
- Ferrara, R.M., Carozzi, M., Di Tommasi, P., Nelsom, D.D., Fratini, G., Bertolini, T., Magliulo, V., Acutis, M., Rana, G., 2016. Dynamics of ammonia volatilization measured by eddy covariance during slurry spreading in north Italy. *Agric. Ecosyst. Environ.* 219, 1–13.
- Finkelstein, P.L., Sims, P.F., 2001. Sampling error in eddy correlation flux measurements. *J. Geophys. Res.* 106, 3503–3509.
- Gu, L., Falge, E.M., Boden, T., Baldocchi, D.D., Black, T., Saleska, S.R., Suni, T., Verma, S. B., Vesala, T., Wofsy, S.C., Xu, L., 2005. Objective threshold determination for nighttime eddy flux filtering. *Agric. For. Meteorol.* 128, 179–197.
- Gu, M., Pan, Y., Walters, W.W., Sun, Q., Song, L., Wang, Y., Xue, Y., Fang, Y., 2022. Vehicular emissions enhanced ammonia concentrations in winter mornings: insights from diurnal nitrogen isotopic signatures. *Environ. Sci. Technol.* 56, 1578–1585.
- He, Y., Pan, Y., Zhang, G., Ji, D., Tian, S., Xu, X., Zhang, R., Wang, Y., 2020. Tracking ammonia morning peak, sources and transport with 1 Hz measurements at a rural site in North China Plain. *Atmos. Environ.* 235, 117630.
- Huo, Q., Cai, X., Kang, L., Zhang, H., Song, Y., Zhu, T., 2015. Estimating ammonia emissions from a winter wheat cropland in North China Plain with field experiments and inverse dispersion modeling. *Atmos. Environ.* 104, 1–10.
- Kljun, N., Calanca, P., Rotach, M.W., Schmid, H.P., 2015. A simple two-dimensional parameterisation for Flux Footprint Prediction (FFP). *Geosci. Model Dev.* 8, 3695–3713.
- Kormann, R., Meixner, F.X., 2001. An analytical footprint model for non-neutral stratification. *Bound. Layer Meteorol.* 99, 207–224.
- Kuang, F.H., Liu, X.J., Zhu, B., Shen, J.L., Pan, Y.P., Su, M.M., Goulding, K., 2016. Wet and dry nitrogen deposition in the central Sichuan Basin of China. *Atmos. Environ.* 143, 39–50.
- Li, Q., Yang, A., Wang, Z., Roelcke, M., Chen, X., Zhang, F., Pasda, G., Zerulla, W., Wissemeyer, A., Liu, X., 2015. Effect of a new urease inhibitor on ammonia volatilization and nitrogen utilization in wheat in north and northwest China. *Field Crop. Res.* 175, 96–105.
- Lian, Z.M., Ouyang, W., Hao, F.H., Liu, H.B., Hao, Z.C., Lin, C.Y., He, M.C., 2018. Changes in fertilizer categories significantly altered the estimates of ammonia volatilizations induced from increased synthetic fertilizer application to Chinese rice fields. *Agric. Ecosyst. Environ.* 265, 112–122.
- Liu, X.J., Duan, L., Mo, J.M., Du, E.Z., Shen, J.L., Lu, X.K., Zhang, Y., Zhou, X.B., He, C.E., Zhang, F.S., 2011. Nitrogen deposition and its ecological impact in China: an overview. *Environ. Pollut.* 159, 2251–2264.
- Liu, X.J., Xu, W., Du, E.Z., Tang, A.H., Zhang, Y., Zhang, Y.Y., Wen, Z., Hao, T.X., Pan, Y. P., Zhang, L., Gu, B.J., Zhao, Y., Shen, J.L., Zhou, F., Gao, Z.L., Feng, Z.Z., Chang, Y. H., Goulding, K., Collett Jr., J.L., Vitousek, P.M., Zhang, F.S., 2020. Environmental impacts of nitrogen emissions in China and the role of policies in emission reduction. *Phil. Trans. R. Soc. A* 378, 20190324.
- Mauder, M., Foken, T., 2015. Documentation and instruction manual of the eddy-covariance software package TK3. *Arbeitsberichte. Universität Bayreuth, Abt. Mikrometeorologie* 62, 1614–8916.
- Mcdermitt, D., Burba, G., Xu, L., Anderson, T., Komissarov, A., Riensche, B., Schedlbauer, J., Starr, G., Zona, D., Oechel, W., Oberbauer, S., Hastings, S., 2011. A new low-power, open-path instrument for measuring methane flux by eddy covariance. *Appl. Phys. B* 102, 391–405.
- McMillen, R.T., 1988. An eddy correlation technique with extended applicability to non-simple terrain. *Bound. Layer Meteorol.* 43, 231–245.
- Milford, C., Theobald, M.R., Nemitz, E., Hargreaves, K.J., Horvath, L., Raso, J., Dammen, U., Neftel, A., Jones, S.K., Hensen, A., Loubet, B., Cellier, P., Sutton, M.A., 2009. Ammonia fluxes in relation to cutting and fertilization of an intensively managed grassland derived from an inter-comparison of gradient measurements. *Biogeosciences* 6, 819–834.
- Moncrieff, J.B., Clement, R., Finnigan, J., Meyers, T., 2004. Averaging, detrending and filtering of eddy covariance time series. In: Lee, X., Massman, W.J., Law, B.E. (Eds.), *Handbook of Micrometeorology: a Guide for Surface Flux Measurements*. Kluwer Academic, Dordrecht, pp. 7–31.
- Moncrieff, J.B., Massheder, J.M., de Bruin, H., Ebers, J., Friborg, T., Heusinkveld, B., Kabat, P., Scott, S., Soegaard, H., Verhoef, A., 1997. A system to measure surface fluxes of momentum, sensible heat, water vapor and carbon dioxide. *J. Hydrol.* 188–189, 589–611.
- Neftel, A., Spirig, C., Ammann, C., 2008. Application and test of a simple tool for operational footprint evaluations. *Environ. Pollut.* 152, 644–652.
- Nemitz, E., Sutton, M.A., Schjørring, J.K., Husted, S., Paul Wyers, G., 2000. Resistance modelling of ammonia exchange over oilseed rape. *Agric. For. Meteorol.* 105, 405–425.
- Pacholski, A., Cai, G., Nieder, R., Richter, J., Fan, X., Zhu, Z., Roelcke, M., 2006. Calibration of a simple method for determining ammonia volatilization in the field—comparative measurements in Henan Province, China. *Nutrient Cycl. Agroecosyst.* 74, 259–273.
- Pan, D., Benedict, K.B., Golston, L.M., Wang, R., Collett, J.L., Tao, L., Sun, K., Guo, X., Ham, J., Prenni, A.J., Schichtel, B.A., Mikoviny, T., Müller, M., Wisthaler, A., Zondlo, M.A., 2021. Ammonia dry deposition in an alpine ecosystem traced to agricultural emission hotspots. *Environ. Sci. Technol.* 55, 7776–7785.
- Pan, Y., Tian, S., Zhao, Y., Zhang, L., Zhu, X., Gao, J., Huang, W., Zhou, Y., Song, Y., Zhang, Q., Wang, Y., 2018. Identifying ammonia hotspots in China using a national observation network. *Environ. Sci. Technol.* 52, 3926–3934.
- Pan, Y., Wang, Y., Tang, G., Wu, D., 2012. Wet and dry deposition of atmospheric nitrogen at ten sites in Northern China. *Atmos. Chem. Phys.* 12, 6515–6535.
- Rannik, Ü., Peltola, O., Mammarella, I., 2016. Random uncertainties of flux measurements by the eddy covariance technique. *Atmos. Meas. Tech.* 9, 5163–5181.
- Sha, Z., Liu, H., Wang, J., Ma, X., Liu, X., Misselbrook, T., 2021. Improved soil-crop system management aids in NH₃ emission mitigation in China. *Environ. Pollut.* 289, 117844.
- Shen, J.L., Tang, A.H., Liu, X.J., Fangmeier, A., Goulding, K.T.W., Zhang, F.S., 2009. High concentrations and dry deposition of reactive nitrogen species at two sites in the North China Plain. *Environ. Pollut.* 157, 3106–3113.
- Sintermann, J., Spirig, C., Jordan, A., Kuhn, U., Ammann, C., Neftel, A., 2011. Eddy covariance flux measurements of ammonia by high temperature chemical ionisation mass spectrometry. *Atmos. Meas. Tech.* 4, 599–616.
- Stull, R.B., 1988. An introduction to boundary layer meteorology. In: *Atmospheric Science Library*. Kluwer, Dordrecht, The Netherlands, p. 666.
- Sun, K., Tao, L., Miller, D.J., Zondlo, M.A., Shonkwiler, K.B., Nash, C., Ham, J.M., 2015. Open-path eddy covariance measurements of ammonia fluxes from a beef cattle feedlot. *Agric. For. Meteorol.* 213, 193–202.
- Tang, Y.S., Simmons, I., van Dijk, N., Di Marco, C., Nemitz, E., Dämmgen, U., Gilke, K., Djuricic, V., Vidic, S., Gliha, Z., Borovecki, D., Mitosinkova, M., Hanssen, J.E., Uggerud, T.H., Sanz, M.J., Sanz, P., Chorda, J.V., Flechard, C.R., Fauvel, Y., Ferm, M., Perrino, C., Sutton, M.A., 2009. European scale application of atmospheric reactive nitrogen measurements in a low-cost approach to infer dry deposition fluxes. *Agric. Ecosyst. Environ.* 133, 183–195.
- Van Damme, M., Clarisse, L., Whitburn, S., Hadji-Lazarou, J., Hurtmans, D., Clerbaux, C., Coheur, P.F., 2018. Industrial and agricultural ammonia point sources exposed. *Nature* 564, 99–103.
- Wang, K., Kang, P., Lu, Y., Zheng, X., Liu, M., Lin, T., Butterbach-Bahl, K., Wang, Y., 2021. An open-path ammonia analyzer for eddy covariance flux measurement. *Agric. For. Meteorol.* 308–309, 108570.
- Webb, E.K., Pearman, G.I., Leuning, R., 1980. Correction of flux measurements for density effects due to heat and water-vapor transfer. *Q. J. Roy. Meteorol. Soc.* 106, 85–100.
- Wen, Z., Xu, W., Pan, X., Han, M., Wang, C., Bebedict, K., Tang, A., Collett Jr., J.L., Liu, X., 2021. Effects of reactive nitrogen gases on the aerosol formation in Beijing from late autumn to early spring. *Environ. Res. Lett.* 16, 025005.

- Wentworth, G.R., Murphy, J.G., Benedict, K.B., Bangs, E.J., Collett, J.L., 2016. The role of dew as a night-time reservoir and morning source for atmospheric ammonia. *Atmos. Chem. Phys.* 16, 7435–7449.
- Werle, P., Miike, R., Slemr, F., 1993. The limits of signal averaging in atmospheric trace gas monitoring by tunable diode-laser absorption spectroscopy (TDLAS). *Appl. Phys. B* 57, 131–139.
- Wesely, M.L., 1989. Parameterization of surface resistances to gaseous dry deposition in regional scale numerical models. *Atmos. Environ.* 23, 1293–1304.
- Wesely, M.L., Hicks, B.B., 1977. Some factors that affect the deposition rates of sulfur dioxide and similar gases on vegetation. *J. Air Pollut. Control Assoc.* 27, 1110–1116.
- Xu, W., Luo, X., Pan, Y., Zhang, L., Tang, A., Shen, J., Zhang, Y., Li, K., Wu, Q., Yang, D., Zhang, Y., Xue, J., Li, W., Li, Q., Tang, L., Lu, S., Liang, T., Tong, Y., Liu, P., Zhang, Q., Xiong, Z., Shi, X., Wu, L., Shi, W., Tian, K., Zhong, X., Shi, K., Tang, Q., Zhang, L., Huang, J., He, C., Kuang, F., Zhu, B., Liu, H., Jin, X., Xin, Y., Shi, X., Du, E., Dore, A., Tang, S., Collett, J., Goulding, K., Sun, Y., Ren, J., Zhang, F., Liu, X., 2015. Quantifying atmospheric nitrogen deposition through a nationwide monitoring network across China. *Atmos. Chem. Phys.* 15, 18365–18405.
- Yang, W., Zhu, A., Chen, X., Zhang, J., Xu, X., Shu, X., 2014. Use of the open-path TDL analyzer to monitor ammonia emissions from winter wheat in the North China Plain. *Nutrient Cycl. Agroecosyst.* 99, 107–117.
- Zhang, L., Moran, M., Makar, P., Brook, J., Gong, S., 2002. Modelling gaseous dry deposition in AURAMS: a unified regional air-quality modelling system. *Atmos. Environ.* 36, 537–560.
- Zhu, X., Shen, J.L., Li, Y., Liu, X.J., Xu, W., Zhou, F., Wang, J., Reis, S., Wu, J.S., 2021. Nitrogen emission and deposition budget in an agricultural catchment in subtropical central China. *Environ. Pollut.* 289, 117870.
- Zhu, Z.L., 1997. Fate and management of fertilizer nitrogen in agroecosystems. In: Zhu, Z.L., Wen, Q.X., Freney, J.R. (Eds.), *Nitrogen in Soils of China*. Kluwer Academic Publishers, Dordrecht, The Netherlands, pp. 239–279.
- Zöll, U., Brümmner, C., Schrader, F., Ammann, C., Ibrom, A., Flechard, C.R., Nelson, D.D., Zahniser, M., Kutsch, W.L., 2016. Surface-atmosphere exchange of ammonia over peatland using QCL-based eddy-covariance measurements and inferential modeling. *Atmos. Chem. Phys.* 16, 11283–11299.